Molecular-dynamics studies of the mixed cyanides. II. Orientational freezing

Laurent J. Lewis
Département de Physique et Groupe de Recherche sur les Couches Minces, Université de Montréal, Case Postale 6128, Succursale A, Montréal, Québec, Canada H3C 3J7

Michael L. Klein
Department of Chemistry, University of Pennsylvania, Philadelphia, Pennsylvania 19104-6323
(Received 1 May 1989)

The technique of constant-pressure molecular dynamics is used to investigate the process of quadrupolar freezing in the mixed cyanide crystals $(KBr)_{1-x}(KCN)_x$. Systems with x larger than the critical concentration $x_c=0.6$ transform to either monoclinic or rhombohedral structures at low temperatures and freeze into a well-defined ferroelastically ordered orientational state. On the other hand, systems with x less than x_c remain cubic at all temperatures and freeze into a state of orientational disorder characterized by a preference for ferroelastic ordering, but with a broad distribution of relative orientations also present. The glass state is found to have characteristics of both the domain and the favored-orientation models.

I. INTRODUCTION

At high temperature, the alkali-cyanide crystals are cubic (space group $Fm3m$), and the CN^- molecular ions undergo rotational diffusion (rotator phase). Orientational glass phases have been observed to develop at low temperatures, and for certain concentrations, in a variety of mixed alkali-cyanides, such as $(NaCN)_{1-x}(KCN)_x$,[1] and alkali-halide/alkali-cyanide mixtures, such as $(KBr)_{1-x}(KCN)_x$,[2-6] $(KCl)_{1-x}(KCN)_x$,[7,8] and $(NaCl)_{1-x}(NaCN)_x$,[9] In the latter group, there exists a critical concentration x_c above which a transition to a low-temperature noncubic structure with long-range orientational order is induced by ferroelastic shear deformations.[10] Below x_c, on the other hand, the inhomogeneous strains of the heavily diluted lattice dominate the ferroelastic strains, causing the long-range orientational order to be lost and the system to freeze into an orientational glass.[2-6] The situation is similar in systems consisting of mixtures of two alkali cyanides, except that the glass-forming range is now determined by two critical concentrations, x_{c_1} and x_{c_2}.[1] The present paper is concerned exclusively with the $(KBr)_{1-x}(KCN)_x$ system.

Upon cooling from the rotator phase, *pure* KCN undergoes a first-order cubic→orthorhombic transition.[11,12] This transition, which occurs at 168 K, is anomalous with T_{2g} phonons exhibiting dramatic softening.[13,14] Coupling between translational and rotational degrees of freedom of the dumbbell-shaped CN^- molecules has been invoked to explain such behavior.[14,15] On substituting the CN^- for Br^-, however, a complex pattern of phases is revealed at low temperatures. For $x>0.85$, orthorhombic and triclinic phases are found to coexist.[5,16,17] For $x_c=0.6<x<0.85$, the ground state is monoclinic,[5,16-18] though a rhombohedral phase is also present at intermediate temperatures.[5,18,19] Finally, at concentrations less than x_c, the crystal remains cubic at all temperatures; ferroelastic anomalies in the dielectric,[20-23] ultrasonic,[22-24] and neutron[2,22,23,25,26] responses, however, reveal that the ground-state structure is a quadrupolar glass.[2,3,27] There is evidence that dipolar (head-to-tail) and quadrupolar (orientational) freezing temperatures differ.[28,29]

In order to rationalize the effect of dilution on the formation of the low-temperature state, we have performed an extensive series of molecular-dynamics (MD) simulations of the mixed alkali-halide/alkali-cyanides.[30-32] One of the conclusions we arrived at was that the ground-state structure of these systems is determined principally by a competition between translation-rotation-mediated CN^--CN^- coupling and coupling of the orientational degrees of freedom of the CN^- molecules to the static random strain fields originating from the chemical disorder of the anion sublattice. (Strains of dynamic origin have also been postulated.)[33] This is consistent with early theoretical work,[34] as well as with recent neutron-diffraction[4] and ultrasonic[35] measurements.

In a previous paper[36] (hereafter referred to as I), we have demonstrated that the simple model used to carry out the simulations—effective two-body interatomic potentials plus a three-site model for the charge distribution of the CN^- molecular ion—could accurately describe the whole structural phase diagram for the $(KBr)_{1-x}(KCN)_x$ system. Here, we give a full account of our findings for the orientational freezing transition, which we only alluded to in I. Thus, consistent with experiment, we find samples with $x>x_c$, which transform to either orthorhombic, monoclinic, or rhombohedral structures at low temperature, to freeze into an orientational *crystal* state, while samples with $x<x_c$, which remain cubic, form an orientational *glass*.

Even though the existence of an orientational glass in samples with $x<0.6$ is now well established, there remain questions regarding the nature of this state.[10,31] Various models have been proposed. Among them are

the "favored-orientation model,"[2,15] where CN^- ions freeze into randomly oriented pockets, e.g., {111}, and the "ferroelastic-domain model,"[10,37] where quadrupoles align within domains, but with disordered wall regions also present. Our MD simulations find the glass-forming systems to exhibit characteristics of both these models though, because of the finite size of our samples, it is not possible to unambiguously resolve the issue. We find a definite preference for neighboring molecules to order ferroelastically (i.e., either parallel or antiparallel), with a "coherence length" of a few interatomic spacings. A broad distribution of relative orientations is also observed, which corresponds to wall regions. This will become clear when we discuss the results of a large simulation we have carried out on a sample with $x=0.50$ at a single temperature, below freezing.

We show in Fig. 1 the real-space trajectory of an individual molecule at two different temperatures, one above and the other below the freezing point. These plots are generated by following, as a function of time, the trace left on the surface of a sphere by the end point of the CN^- molecule. (Only the northern hemisphere is shown, as we use periodic boundary conditions across the equator.) Thus, at high temperature, where the molecule undergoes rotational diffusion, the trajectory resembles a random walk. At low temperature, however, the molecule clearly freezes into a well-defined direction ([111], as we will see later), and undergoes small-amplitude librational motion. Though such plots provide an interesting visual illustration of the frozen-in configurations of individual molecules, they are not practical in assessing the collective features of the freezing transition. In the following, we present a detailed analysis of our simulation in terms of configuration-averaged individual CN^- ions orientational order parameters, as well as in terms of the relative ordering between neighboring pairs of molecules.

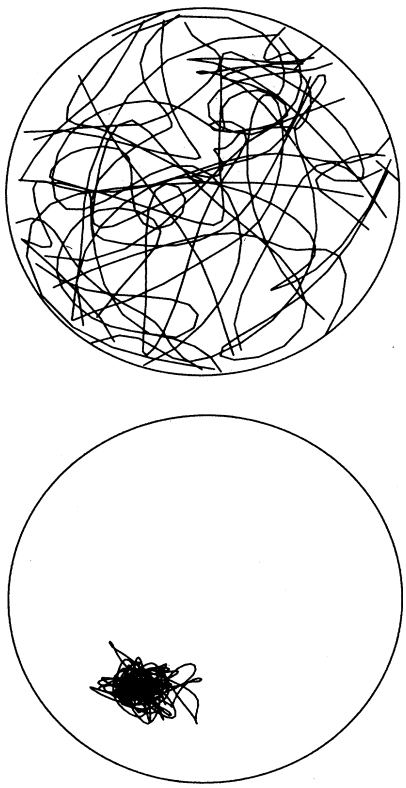

FIG. 1. Real-space trajectories of an individual CN^- molecule in the high-temperature rotator phase (top) and in the frozen-in low-temperature state (bottom—here, the molecule is librating about the [111] direction). Details are given in the text.

Our MD simulations were performed in the isobaric-isoenthalpic (N,P,H) ensemble,[38–40] and employed neutral, periodically replicated systems consisting each of $N=512$ ions. The room-temperature cubic rotator phase was set up using in each case the known value of the lattice parameter, and the equations of motion for the ions were integrated using standard techniques. The ions interacted via model-potential functions taken from previous studies of the alkali cyanides.[41–46] The effect of isobarically cooling each sample was then monitored. At each temperature, the trajectories of all particles were followed over 3500–5000 timesteps of 2 fs each, with the first 500 reserved for equilibration. Full details of the calculations can be found in I, together with a set of tables giving, for each run, the system's energy and volume as a function of temperature.

The remainder of this paper is organized as follows. First, in Sec. II, we discuss orientational freezing in samples which form ordered pattern at low temperature. A corresponding analysis is presented in Sec. III for systems in the glass-forming range of concentrations. For completeness, we briefly discuss in Sec. IV the site-ordered systems introduced in I. Conclusions are given in Sec. V.

II. ORDERING PHASES

The orientational freezing process can be monitored in terms of the order parameters introduced by Edwards and Anderson[47] to treat the problem of magnetic impurities in spin glasses. Thus, following Michel and Rowe,[3] we examine functions of the molecular orientations having the form $[\langle Y(\hat{\mathbf{u}})\rangle]$, and their fluctuations, $\{[\langle Y(\hat{\mathbf{u}})\rangle^2]\}^{1/2}$, where $\langle\cdots\rangle$ denotes a time average for an individual CN^- ion, and $[\cdots]$ an average over all sites. Here, $\hat{\mathbf{u}}\equiv(x,y,z)$ is the unit vector along the C—N bond; the cubic crystal axes are used as reference frame. Dipolar (D) order is described via the three functions

$$Y_1^{(1)}=\sqrt{3/4\pi}x\ ,\quad Y_2^{(1)}=\sqrt{3/4\pi}y\ ,\quad Y_3^{(1)}=\sqrt{3/4\pi}z\ , \tag{1}$$

whereas quadrupolar order is described via two functions of E_g symmetry,

$$Y_1^{(2)}=\sqrt{15/4\pi}(3z^2-1)\ ,\quad Y_2^{(2)}=\sqrt{15/4\pi}(x^2-y^2)\ , \tag{2}$$

and three functions of T_{2g} symmetry,

$$Y_3^{(2)} = \sqrt{15/4\pi}\,xy \ ,$$
$$Y_4^{(2)} = \sqrt{15/4\pi}\,yz \ , \tag{3}$$
$$Y_5^{(2)} = \sqrt{15/4\pi}\,zx \ .$$

Figure 2 shows the temperature dependence of these parameters for the sample with $x=0.73$. From I, we recall that this system transforms to either monoclinic (run labeled I) or rhombohedral (labeled II) on cooling from the high-temperature cubic rotator phase. We consider run II first because it is easier to understand. From the fluctuations of the order parameters, it is clear that at low temperature the CN^- have frozen-in orientations with quadrupoles ordering essentially along $\{111\}$ directions. Perfect $\{111\}$ order would yield $\{[\langle D\rangle^2]\}^{1/2}=0.282$, $\{[\langle E_g\rangle^2]\}^{1/2}=0$, and $\{[\langle T_{2g}\rangle^2]\}^{1/2}=0.364$; the E_g fluctuation is, however, a very sensitive measure of the mean-square angular displacement (librational motion) of the molecule about its equilibrium orientation—here perfect $\{111\}$.

Unfortunately, the fluctuations cannot distinguish between cases where CN^- ions freeze into $\{111\}$ pockets at random (i.e., uncorrelated), or well-defined $\{111\}$ pockets (i.e., correlated). This can, however, be resolved by examining the other quantities plotted in Fig. 2. While the value of $[\langle D\rangle]$ indicates that head-to-tail disorder is present (the net dipole moment of the sample is zero), it can be inferred from the behavior of $[\langle T_{2g}\rangle]$ that *only* the [111] and $[\bar{1}\bar{1}\bar{1}]$ directions are occupied. Thus, quadrupoles have ordered with C—N bond vectors essentially parallel to the [111] direction of the parent cubic phase (that is along the rhombohedral axis), but with head-to-tail disorder (i.e., antiferroelectrically, in an average sense; the time scale of true dipole ordering[28] is far beyond the reach of present simulations). Note in Fig. 2 the remarkably rapid increase of the $[\langle T_{2g}\rangle]$ parameter starting at a temperature of about 125 K. This marks the onset of the orientational freezing transition. We will return to this point below.

The corresponding order parameters for run I exhibit different behavior. While the fluctuations again indicate that dipoles align along $\{111\}$ directions, it is clear from the $[\langle T_{2g}\rangle]$ parameter that the orientational order is not the same here as in run II. We can find no simple interpretation for this behavior. To resolve the issue, we consider, in Figs. 3 and 4, selected "slices" through the periodically replicated MD cell and plot, for each, the projection of all CN^- molecular-bond vectors whose center of mass resides in that plane (we do not distinguish here between head and tail). Note in Figs. 3 and 4, that the *same* set of planes is displayed for the two runs. Thus, as was already clear from our discussion above, run II freezes in a unique direction, namely [111], while run I exhibits a separation into two domains of comparable dimension. This explains our findings for the order parameters for this system, Fig. 2, which results from the convolution of two distinct (but parent) directions of freezing. This effect, however, should not be taken too seriously, as it is most likely a consequence of the finite size of our MD sample and of too rapid a quench rate (cf. I). It is nevertheless interesting to see it emerge from the simulation. Such plots are most useful in discriminating between various models for the orientational glass state, as discussed in Sec. III.

Information about the orientational probability distribution $F(\hat{\mathbf{u}})$ can also be obtained from its expansion in

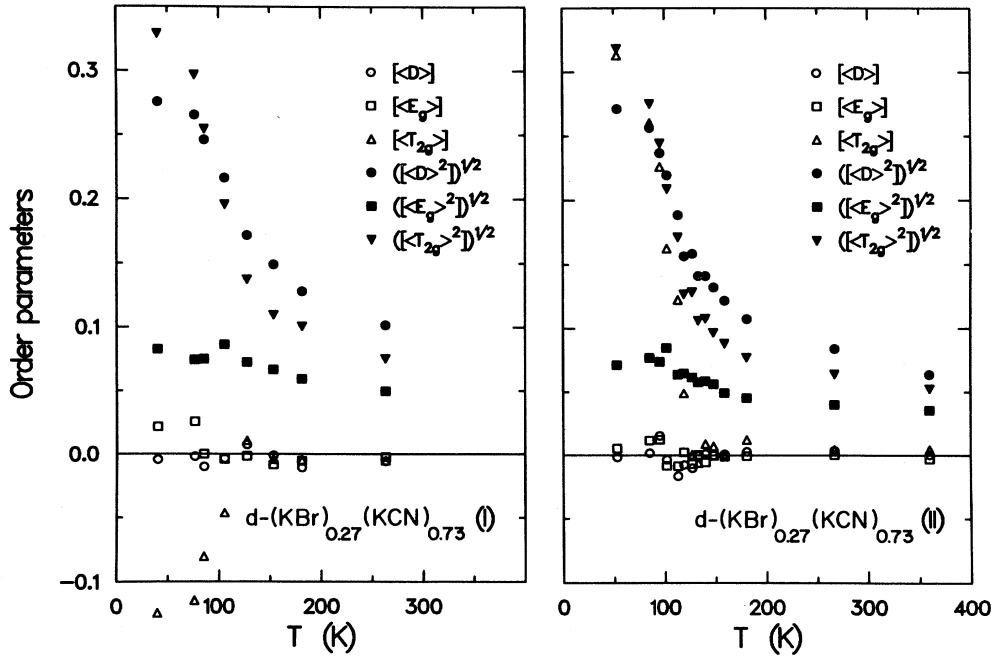

FIG. 2. Temperature dependence of the CN^- Edwards-Anderson-type orientational order parameters, Eqs. (1)–(3), for the $(KBr)_{0.27}(KCN)_{0.73}$ sample, runs I and II.

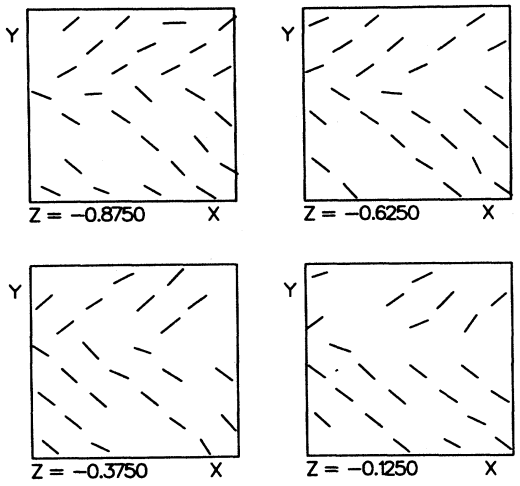

FIG. 3. Selected slices through the $(KBr)_{0.27}(KCN)_{0.73}$ sample, run I, at low temperature, showing the orientations of individual CN^- molecules. Br^- and K^+ ions are omitted for clarity; see text for details.

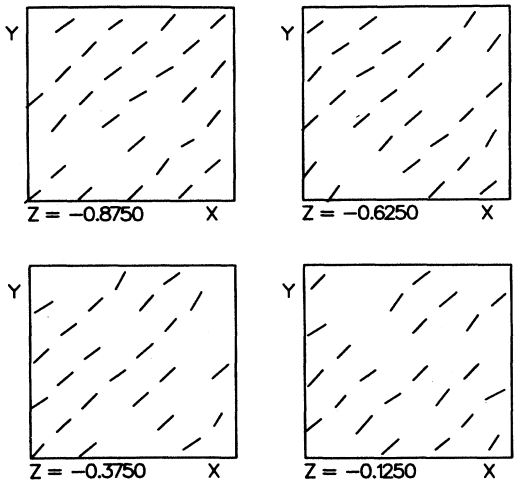

FIG. 4. Same as Fig. 3, but for run II of the $x=0.73$ sample.

terms of kubic harmonics:

$$4\pi F(\hat{\mathbf{u}})=1+C_4K_4+C_6K_6+\cdots\ , \tag{4}$$

where

$$C_4=\langle K_4\rangle=\sqrt{21/16}\langle 5(x^4+y^4+z^4)-3\rangle$$

and

$$C_6=\langle K_6\rangle=\sqrt{13/128}\langle 21(x^4+y^4+z^4)+462x^2y^2z^2-17\rangle\ .$$

These coefficients are of particular interest since they can be determined from neutron-diffraction[11,12] as well as nuclear magnetic resonance[48] experiments. They are shown in Fig. 5. Just like the fluctuations in Fig. 2, those parameters are not sensitive to the specific directions along which the molecules align, and both systems exhibit similar behavior. At high temperature, C_4 approaches zero from the negative side, characteristic of a state of rotational diffusion with, perhaps, a slight preference for $\{111\}$ directions. This preference in ordering becomes unambiguous at low temperature, with C_4 taking a strongly negative value, of the order of -1; perfect $\{111\}$ order would yield $C_4=-1.53$. Similar conclusions can be inferred from the temperature dependence of C_6, for which perfect $\{111\}$ yields $C_6=+2.27$. Though it is perhaps difficult to assess from this graph, C_4 and C_6

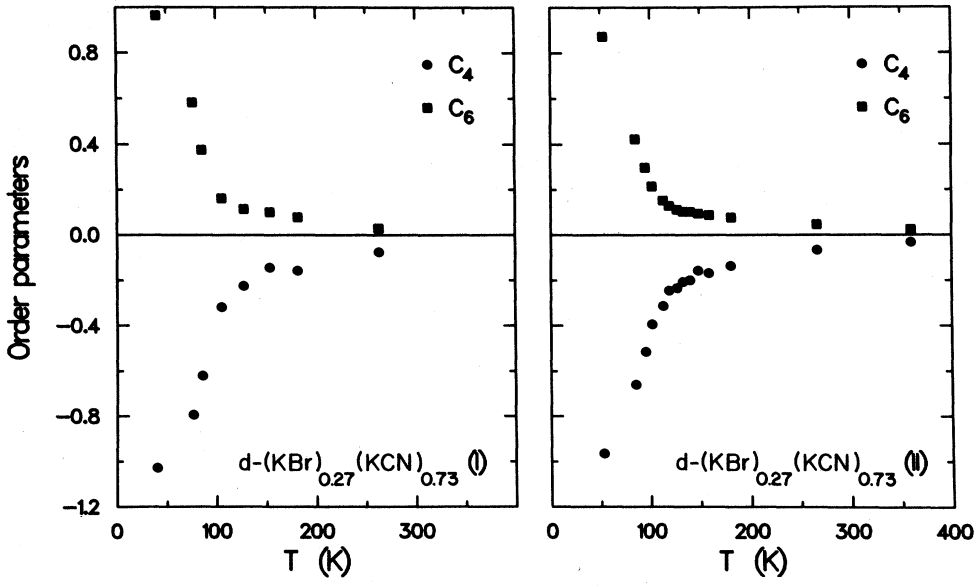

FIG. 5. Temperature dependence of the kubic-harmonics expansion coefficients of the orientational probability function $F(\hat{\mathbf{u}})$, Eq. (4), for the $(KBr)_{0.27}(KCN)_{0.73}$ sample, runs I and II.

seem to exhibit a discontinuous change in slope at $T \approx 125$ K, a temperature we earlier identified as the onset of the orientational freezing transition, and which corresponds to the *structural* transition from the cubic to the rhombohedral phase. In *pure* KCN, C_4 is experimentally[11] found to take values of -0.13 and -0.02 at $T=295$ and 180 K, respectively, while $C_6=+0.23$ and $+0.22$. The behavior of C_4 has been interpreted[11] as evidence for a weak preference for [111] orientation at room temperature, and a slight shift towards [001] at lower temperature. We do not observe this trend here, C_4 becoming increasingly negative as cooling proceeds (though it is possible that the change in slope at 125 K is a manifestation of the experimentally observed behavior). This may indicate a failure of our rigid-ion model in predicting the microscopic details of orientational freezing.

We now examine *correlations* between the orientations of neighboring CN^- molecules. Though such an analysis is most useful in elucidating the nature of the *glass* state, we present it here to allow comparison with corresponding data which will be presented in Sec. III. The quantity we calculate is $P_1(\cos\theta)$, which gives the relative probability of finding a pair of *first*-neighbor CN^- molecules such that θ is the angle between them. The temperature dependence of $P_1(\cos\theta)$ for run II is displayed in Fig. 6—results for run I are comparable (*modulo* the differences discussed above) and are therefore not shown. At high temperature, where the system is in a state of rotational diffusion, the molecules interact with one another only weakly (i.e., they behave as independent rotors), and there is no preferred orientation: The distribution is flat. As cooling proceeds, however, a tendency develops for neighboring molecules to align with their axes parallel ($\cos\theta=+1$) or antiparallel ($\cos\theta=-1$) with equal probability so that the net dipole moment of the sample vanishes. At the lowest temperature, those peaks at $\cos\theta=\pm1$ become extremely sharp (note that the lowest two panels in Fig. 6 have been scaled down by a factor of 5) and no other relative orientation is possible: The quadrupoles have *completely* ordered in a ferroelastic pattern. The point at which $P_1(\cos\theta)$ "touches" the axis of abscissa (here ≈ 90 K) can be taken as the freezing temperature. The system passes from a state of dynamic orientational disorder at high temperature to one of dynamic *and* static order at low temperature.

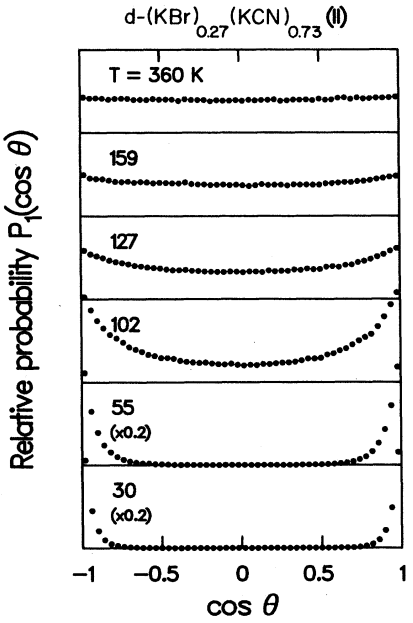

FIG. 6. The function $P_1(\cos\theta)$, which gives the relative probability of finding pairs of nearest-neighbor molecules such that θ is the angle between them, for the $(KBr)_{0.27}(KCN)_{0.73}$ sample, run II, at various temperatures. Note that the lowest two panels have been scaled down for clarity.

The dynamical aspects of the freezing transition can be described in more detail by monitoring the angular diffusion constant D_Ω as well as the single-ion ("self-") reorientation times relevant to NMR experiments, τ^s_{11} and τ^s_{33}, defined as:

$$\tau^s_{\alpha\alpha}=\frac{1}{R^s_{\alpha\alpha}}\int_0^\infty R^s_{\alpha\alpha}(t)dt \ , \tag{5}$$

where

$$R^s_{11}(t)=\langle Y^{(2)}_1(t)Y^{(2)}_1(0)\rangle \quad (E_g) \ , \tag{6}$$

$$R^s_{33}(t)=\langle Y^{(2)}_3(t)Y^{(2)}_3(0)\rangle \quad (T_{2g}) \ . \tag{7}$$

These constitute the only time-correlation functions of interest for a diatomic molecular ion in a cubic crystal field. They are shown in Fig. 7—again only for the $x=0.73$ run II sample. Experimentally, the quantity measured is

$$\tau_2=\tfrac{2}{5}[1+(3/\sqrt{21})C_4]\tau^s_{11}+\tfrac{3}{5}[1-(2/\sqrt{21})C_4]\tau^s_{33} \ .$$

In pure KCN, $\tau_2=0.16$ and 0.33 ps at 294 and 193 K, respectively.[49] Agreement is only fair here, and this is likely a consequence of the simple nature of our model. However, our calculations lead to the same tendency, namely τ^s_{11} and τ^s_{33} increase on cooling. The fact that they seem to diverge indicates that orientational freezing has taken place on the time scale of the MD experiment. This is also clear from the angular diffusion constant, which shows a sharp transition to occur at about 80 K.

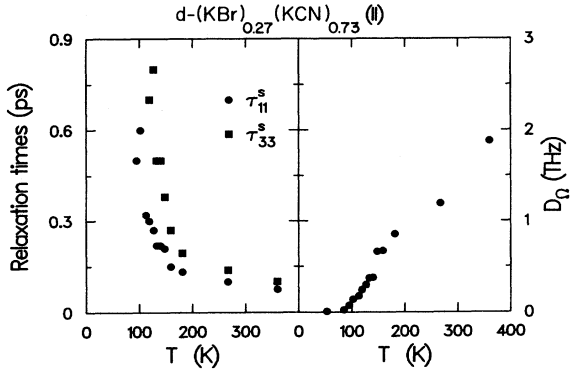

FIG. 7. Temperature dependence of the single-ion reorientation times τ^s_{11} and τ^s_{33} and angular diffusion constant D_Ω for the $(KBr)_{0.27}(KCN)_{0.73}$ mixture, run II.

By comparison, orientational glass formers exhibit a more gradual approach to the transition.

III. GLASS-FORMING PHASES

Orientational glass formers, which exhibit a disordered pattern of molecular orientations at low temperatures, were examined at two values of the cyanide concentration, namely $x=0.50$ and 0.25. In accord with experiment, both systems are found to remain cubic at all temperatures (cf. I). Figure 8 shows the Edwards-Anderson order parameters for the two samples. They exhibit similar behavior except that the transition is shifted to lower temperature in the system with $x=0.25$, as also observed experimentally. Note the relatively important scatter in the points, particular evident in the $x=0.25$ sample, which arises from poorer statistics due to the smaller number of CN^- molecules employed in the calculation.

It is clear, upon comparing with corresponding results for the orientational crystal phases, Fig. 2, that samples with $x<x_c$ are different. Here, as indicated by the values of $\{[\langle D\rangle^2]\}^{1/2}$ and $\{[\langle T_{2g}\rangle^2]\}^{1/2}$, CN^- axes again align along $\{111\}$ directions, *but only in an average sense:* the large value of $\{[\langle E_g\rangle^2]\}^{1/2}$ here signals substantial departures from this particular direction. In fact, as can be deduced from the values of the other order parameters in Fig. 8, the distribution of orientations is fairly wide, though the samples again have vanishing dipole moments. These results already suggest that these systems have frozen into the orientational-glass state.

In order to ascertain this, we again examine the CN^- near-neighbor orientational correlation function $P_1(\cos\theta)$. This is shown in Fig. 9. At high temperature, both systems are in a state of rotational diffusion, and the distribution is flat. As cooling proceeds, the tendency observed earlier for neighboring molecules to align with their axes parallel or antiparallel again develops. However, at the lowest temperature, in distinct contrast with the situation in $(KBr)_{0.27}(KCN)_{0.73}$, there still exists, superimposed on the two peaks at $\cos\theta=\pm1$ (which account for about 30% of the calculated spectrum), a broad more or less featureless background of relative orientations. Further cooling is not likely to affect the situation significantly since orientational freezing has already taken place at this point (at least on the same scale of the MD experiment). We have, however, tested the time dependence of our results for the frozen-in state of the $(KBr)_{0.75}(KCN)_{0.25}$ sample by extending the run at 25 K from 6 to 16 ps, and recomputing $P_1(\cos\theta)$. This is shown in Fig. 10. We find essentially no difference between the two runs, the small discrepancies being most probably due to statistical error. Thus, even on the shorter of the two time scales (which are relevant to neutron-scattering experiments), the system is frozen, i.e., relaxation processes have ceased. The system is therefore in a state of "structural arrest," a state we might call an orientational glass. It is not clear which orientational configurations give rise to the broad low-temperature background in Fig. 9, though we have been able to identify contributions from particular $\{111\}$ directions correlated with $\{110\}$, $\{100\}$, and other $\{111\}$ directions. It is interesting to note that ideal quadrupolar (i.e., perpendicular) ordering is *not* a particularly favorable configuration.

Further insights into the nature of the orientational glass state can, however, be gained by examining in-plane

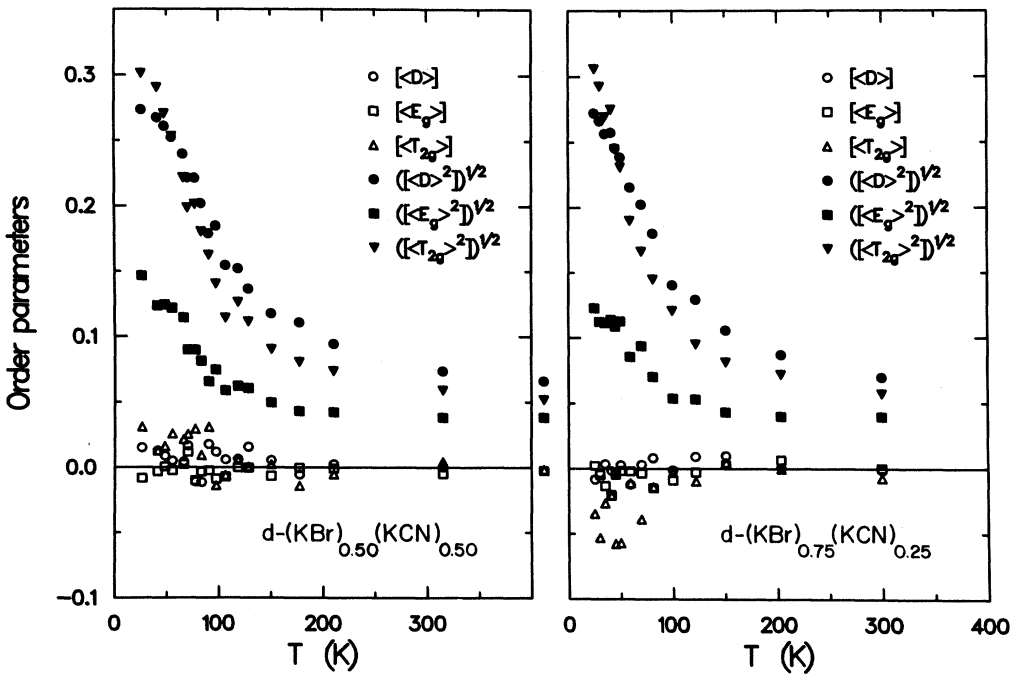

FIG. 8. Same as Fig. 2, but for the orientational glass formers $(KBr)_{0.5}(KCN)_{0.5}$ and $(KBr)_{0.75}(KCN)_{0.25}$.

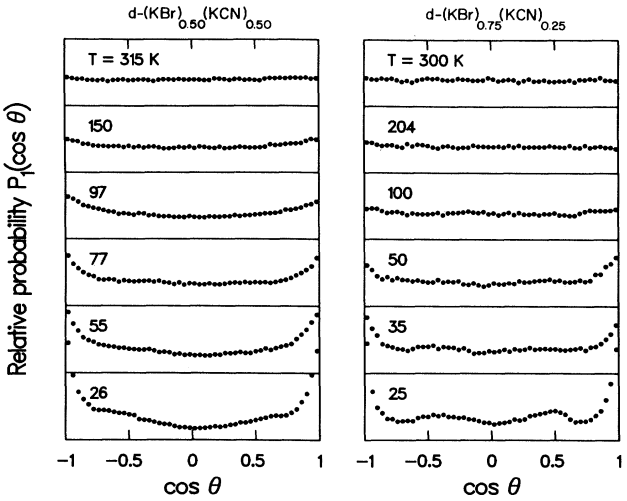

FIG. 9. Same as Fig. 6, but for the $(KBr)_{0.5}(KCN)_{0.5}$ and $(KRr)_{0.75}(KCN)_{0.25}$ samples.

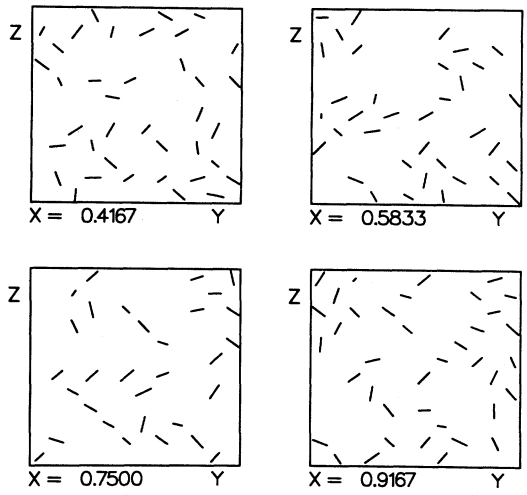

FIG. 11. Same as Fig. 3, but for the $x=0.5$ system; note here that the MD cell consists of $6\times6\times6$ unit cells.

projections of the molecular direction vectors, as was done for $(KBr)_{0.27}(KCN)_{0.73}$ (cf. Figs. 3 and 4). In the course of a different but related study, a system with $x=0.50$ consisting of $6\times6\times6$ unit cells (rather than $4\times4\times4$) was examined though because of the excessive demands on computer resources, at only one temperature, below freezing. Typical "slices" through this system are shown in Fig. 11. One must recall, when examining such pictures, that periodic boundary conditions are employed in our simulations. Correlations between molecules on either side of a boundary therefore exist. (In Fig. 11, only the actual MD cell is shown, i.e., not its replicas.) Also, the planes represented in fact lie on top of one another. Although it is difficult here to describe the frozen-in configuration using the language of domains and domain walls, it is clear that there exists significant regions of ferroelastic order, which extend over a few interatomic spacings, and which seem to be destroyed by the presence of voids in the structure. A fair proportion of the CN^- molecules do not follow this pattern, however, and choose to sit in apparently random orientations.

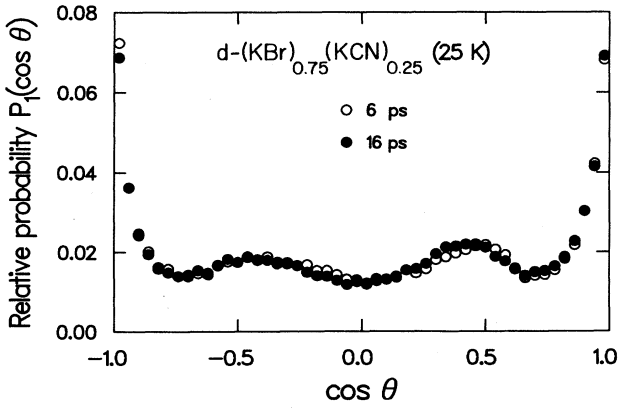

FIG. 10. Time dependence of $P_1(\cos\theta)$ in the orientational glass phase of $(KBr)_{0.75}(KCN)_{0.25}$.

Thus, the orientational glass state appears to possess characteristics of *both* the favored-orientation model,[2,15] and the model which advocates the existence of domains of preferred orientations.[10,37] Figure 11 illustrates in an interesting manner the concept of random fields in these systems.

We now monitor the glass transition more closely in terms of the static and dynamic order parameters described in Sec. II. Figure 12 shows the temperature dependence of the quantities C_4 and C_6, which yield information about the orientational distribution function, while Fig. 13 shows the NMR relaxation times τ^s_{11} and τ^s_{33}, as well as the angular diffusion constant D_Ω. Though C_4 and C_6 convey information similar to that given by Fig. 8, we discuss them here for completeness, and also because they exhibit interesting behavior near the transition. In both cases, C_4 and C_6 vanish in the high-temperature rotator phase, and freeze to some large value at low temperature, corresponding, again only in an average sense, to {111} ordering. In the $(KBr)_{0.5}(KCN)_{0.5}$ mixture, however, the data points exhibit notable dispersion, which suggest that a complicated transitional sequence is taking place. In particular, there appears to exist a discontinuity in the C_4 parameter, which we already noted in the $x=0.73$ sample, at a temperature *somewhat above* the freezing point for this system ($T_g\approx50$ K, cf. Fig. 13). That the transition is more complicated in $(KBr)_{0.5}(KCN)_{0.5}$ than in $(KBr)_{0.75}(KCN)_{0.25}$ is not surprising since, being closer to the critical concentration $x_c=0.6$, the former experiencess more severely the effect of random strain fields which couple to the orientational motion of the cyanide molecules. This is in fact entirely in line with our findings for the temperature dependence of the *structural* parameters (cf. I), which also exhibit substantial dispersion effects at a temperature above orientational freezing. This temperature corresponds to the point where the net coupling between the CN^- orientational degrees of freedom and phonons or strains is at a maximum. It also coincides with the structural transfor-

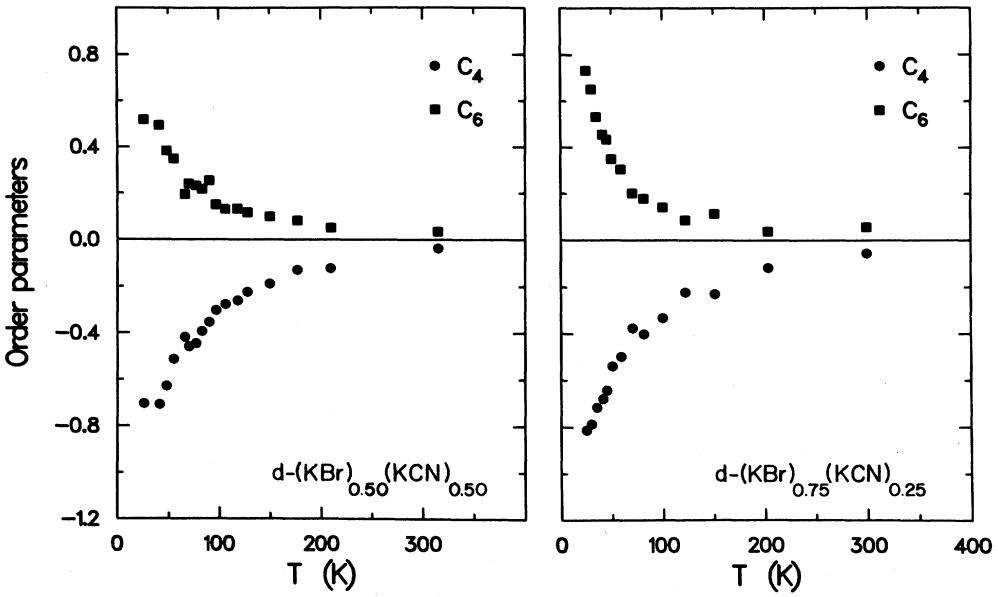

FIG. 12. Same as Fig. 5, but for the $(KBr)_{0.5}(KCN)_{0.5}$ and $(KBr)_{0.75}(KCN)_{0.25}$ samples.

mation and, therefore, maximum anomalous acoustic behavior.[36] The discontinuity in C_4 observed in our calculations can, therefore, be regarded as a precursor signal to the quadrupolar freezing transition.

Experimentally, neutron-scattering[11,12] and NMR[48] measurements suggest that the CN^- orientational probability distribution has a *minimum* along [111], and the value of C_4 is correspondingly positive. This, again, may reveal a relative inadequacy of our model. However, it may also be related to the small run time, i.e., large cooling rate, used in the simulations. It is conceivable that, on the MD time scale, the system is in fact in metastable equilibrium; the break in C_4 noted above may be related to this. A detailed analysis of the time dependence of C_4 and of the full probability distribution $F(\hat{\mathbf{u}})$ is, however, needed to clarify this point.

Finally, upon comparing the values of the angular diffusion constant D_Ω obtained here with the corresponding ones for the $(KBr)_{0.27}(KCN)_{0.73}$ mixture, Fig. 7, we observe that the freezing transition is more sharply defined in the latter than in the former. Freezing is approached more gradually in the glass-forming samples, and the transition appears to be continuous. This behavior is characteristic of glasses. NMR experiments on a sample with $x=0.50$ seem to confirm the continuous nature of the transition.[29]

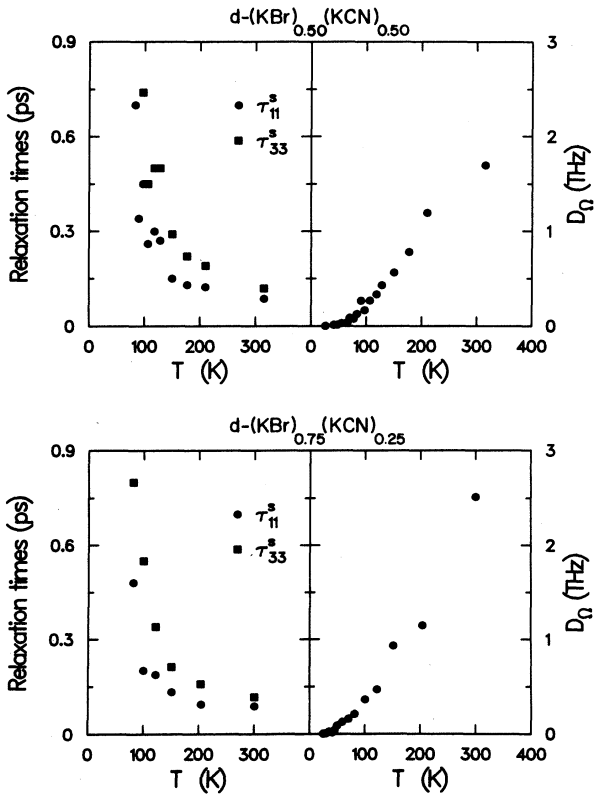

FIG. 13. Same as Fig. 7, but for the $(KBr)_{0.5}(KCN)_{0.5}$ and $(KBr)_{0.75}(KCN)_{0.25}$ samples.

IV. SITE-ORDERED PHASES

Site-ordered mixtures, where the CN^- and Br^- sit in a regular fashion on the anion sublattice, were investigated in I in order to isolate the effects of strain-rotation coupling from those of translation-rotation coupling. Since such systems are most interesting in the study of structural transformations (and since they are really fictitious), we only briefly discuss them here. Further, because it is isomorphous to common A_3B-type alloys, we concentrate on the sample with $x=0.75$.

Orientational freezing is monitored as before in terms of τ_{11}^s, τ_{33}^s, and D_Ω in Fig. 14 and C_4 and C_6 in Fig. 15. Thus, the transition occurs at ≈ 90 K here, as evident from the angular diffusion constant. However, C_4 and C_6 again, and perhaps even more clearly, exhibit peculiar behavior, at a temperature above freezing, namely ≈ 120

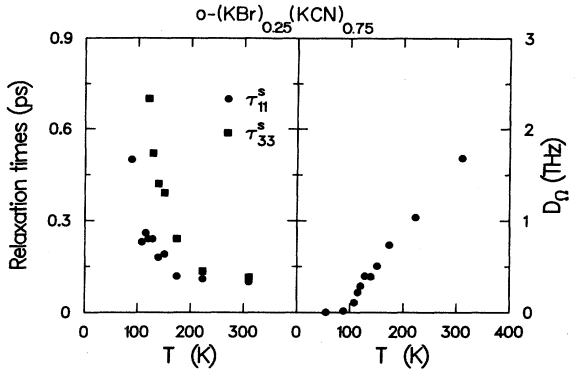

FIG. 14. Same as Fig. 7, but for the site-ordered $x=0.75$ sample.

K. Both parameters go through a change in slope at this temperature; this is particularly marked in C_4. Since random strains are (presumably) absent from this system, we can only conclude that it is the coupling of the orientational with the *translational* degrees of freedom of the CN^- molecules which is responsible for the anomaly, and it may in fact simply be a manifestation of steric hindrance. The anomaly is stronger here than in the corresponding site-disordered systems. It is, therefore, tempting to conjecture that the effect of random strains, by analogy with topological glasses, is to broaden the freezing transition, which then becomes continuous in the orientational glass-forming samples. This point, however, deserves further investigation.

Because they possess a high degree of symmetry, site-ordered systems naturally freeze into well-ordered orientational phases at low temperature. This is shown in Fig. 16 where we plot $P_1(\cos\theta)$, the relative orientational probability function. Thus again, the high-temperature phase is in a state of relatively free rotational diffusion. As cooling proceeds, wings develop which correspond to parallel and antiparallel alignment of neighboring molecules. The pattern of order is completely static at the lowest temperature and is shown in Fig. 17. (Note that the periodicity of this system is twice that of pure KCN.)

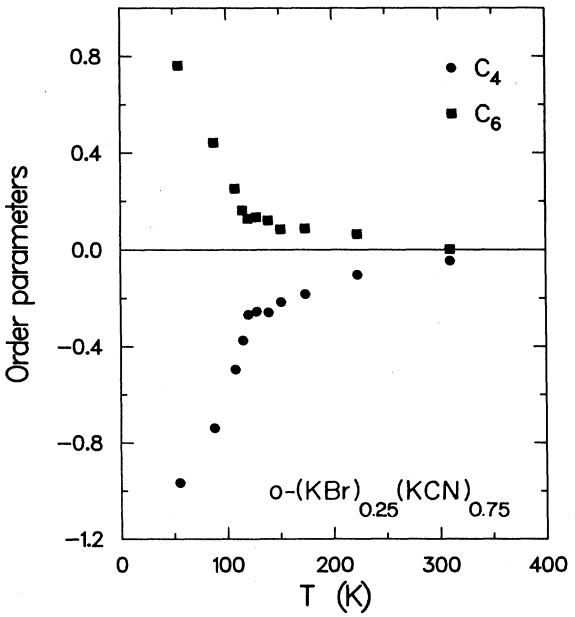

FIG. 15. Same as Fig. 5, but for the site-ordered $x=0.75$ mixture.

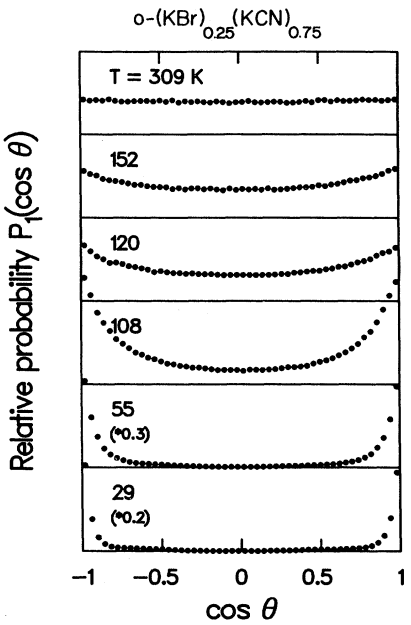

FIG. 16. Same as Fig. 6, but for the site-ordered $x=0.75$ mixture.

V. CONCLUSIONS

We have used molecular dynamics to investigate the process of quadrupolar freezing in $(KBr)_{1-x}(KCN)_x$ mix-

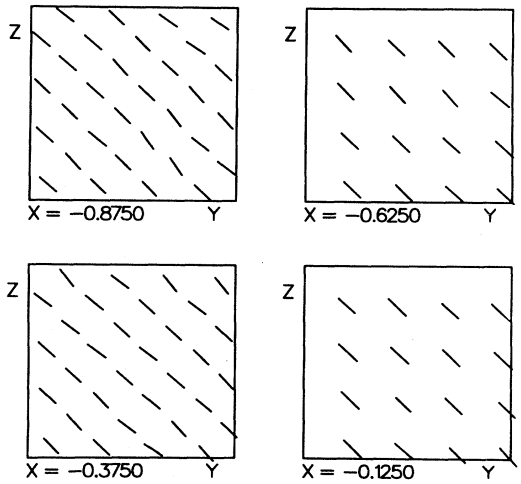

FIG. 17. Same as Fig. 3, but for the site-ordered $x=0.75$ mixture.

tures. A sample with $x=0.73$, which transforms from cubic to either monoclinic or rhombohedral at low temperature, is found to freeze into a well-defined pattern of orientations, with ferroelastic order along specific directions, but with dipolar (head-to-tail) disorder. By contrast, samples with $x=0.50$ and 0.25, i.e., below the critical concentration x_c, remain cubic at all temperatures and freeze into a state of orientational disorder.

Though a detailed analysis of the relative orientational distribution function in the glass state reveals a distinct preference for ferroelastic ordering, a broad contribution also exists which corresponds to more or less random arrangements of the CN^- molecules. Ideal quadrupolar ordering, where the orientations of neighboring molecules are perpendicular, is not a favorable configuration.

One of the aims of this work was to provide insights into the nature of the orientational glass state. Though the conclusions that can be drawn from our simulations are somewhat limited by the finite size of the MD sample, this state is found to possess characteristics of both models which have been proposed for it. Thus, it appears that "domains" extending over a few lattice spacings form in which quadrupoles align along preferential directions. These are separated by regions which could be regarded as "walls," where orientations are again mostly along preferential directions, but neighboring molecules are essentially uncorrelated. The extent and number of the domains seems to be principally determined by the presence of voids (i.e., sites occupied by a Br^- ion rather than a CN^- molecule) in the structure. Thus, the domain picture is perhaps more appealing in glass-forming systems at concentrations close to x_c, while systems with $x \rightarrow 0$ are best described in terms of the preferred-orientation model.

We have not discussed here the detailed time dependence of the molecules collective motions and, in particular, the relaxation processes they undergo. Such interesting questions remain for future investigations.

ACKNOWLEDGMENTS

We thank J.-F. Berret, M. S. Conradi, S. Galam, C. W. Garland, K. Knorr, A. Loidl, K. H. Michel, J. M. Rowe, and D. Walton for many enlightening discussions, and R. W. Impey for invaluable assistance with numerous computational aspects of this work. The research described herein was supported by the National Research Council of Canada, by the Natural Sciences and Engineering Research Council of Canada, and by the U.S. National Science Foundation. Finally, we also thank Cray Canada, Inc. for a generous allocation of CPU time.

[1]A. Loidl, T. Schräder, R. Böhmer, K. Knorr, J. K. Kjems, and R. Born, Phys. Rev. B **34**, 1238 (1986).
[2]J. M. Rowe, J. J. Rush, D. G. Hinks, and S. Susman, Phys. Rev. Lett. **43**, 1158 (1979).
[3]K. H. Michel and J. M. Rowe, Phys. Rev. B **22**, 1417 (1980).
[4]A. Loidl, K. Knorr, J. M. Rowe, and G. J. McIntyre, Phys. Rev. B **37**, 389 (1988).
[5]J. Ortiz-Lopez and F. Luty, Phys. Rev. B **37**, 5461 (1988).
[6]J. Ortiz-Lopez and F. Luty, Phys. Rev. B **37**, 5452 (1988).
[7]D. Durand and F. Luty, Ferroelectrics **16**, 205 (1977); J. C. Castro and M. de Souza, Phys. Status Solidi B **86**, 137 (1978).
[8]K. Knorr and A. Loidl, Phys. Rev. Lett. **57**, 460 (1986).
[9]S. Elschner, K. Knorr, and A. Loidl, Z. Phys. B **61**, 209 (1985).
[10]K. Knorr, E. Civera-Garcia, and A. Loidl, Phys. Rev. B **35**, 4998 (1987); K. Knorr, U. G. Volkmann, and A. Loidl, Phys. Rev. Lett. **57**, 2544 (1986).
[11]J. M. Rowe, D. G. Hinks, D. L. Price, S. Susman, and J. J. Rush, J. Chem. Phys. **58**, 2039 (1973).
[12]J. M. Rowe, J. J. Rush, and E. Prince, J. Chem. Phys. **66**, 5147 (1977).
[13]S. Haussühl, Solid State Commun. **13**, 147 (1973).
[14]J. M. Rowe, J. J. Rush, N. Chesser, K. H. Michel, and J. Naudts, Phys. Rev. Lett. **40**, 455 (1978).
[15]K. H. Michel and J. M. Rowe, Phys. Rev. B **32**, 5827 (1985).
[16]J. M. Rowe, J. J. Rush, and S. Susman, Phys. Rev. B **28**, 3506 (1983).
[17]J. M. Rowe, J. Bouillot, J. J. Rush, and F. Luty, Physica (Amsterdam) **136B**, 498 (1986).
[18]K. Knorr and A. Loidl, Phys. Rev. B **31**, 5387 (1985).
[19]K. Knorr, A. Loidl, and J. K. Kjems, Phys. Rev. Lett. **55**, 2445 (1985); see also Physica (Amsterdam) **136B**, 311 (1986).
[20]S. Bhattacharya, S. R. Nagel, L. Fleishman, and S. Susman, Phys. Rev. Lett. **48**, 1267 (1982).
[21]K. Knorr and A. Loidl, Z. Phys. B **46**, 219 (1982).
[22]A. Loidl, R. Feile, and K. Knorr, Phys. Rev. Lett. **48**, 1263 (1982).
[23]R. Feile, A. Loidl, and K. Knorr, Phys. Rev. B **26**, 6875 (1982).
[24]C. W. Garland, J. Z. Kwiecien, and J. C. Damien, Phys. Rev. B **25**, 5818 (1982); J. Z. Kwiecien, R. C. Leung, and C. W. Garland, *ibid.* **23**, 4419 (1981).
[25]A. Loidl, R. Feile, K. Knorr, and J. K. Kjems, Phys. Rev. B **29**, 6052 (1984).
[26]A. Loidl, R. Feile, K. Knorr, B. Renker, J. Daubert, D. Durand, and J.-B. Suck, Z. Phys. B **38**, 253 (1980).
[27]K. Knorr, Phys. Scr. T **19**, 531 (1987).
[28]U. G. Volkmann, B. Böhmer, A. Loidl, K. Knorr, U. T. Höchli, and S. Haussühl, Phys. Rev. Lett. **56**, 1716 (1986).
[29]M. A. Doverspike, M.-C. Wu, and M. S. Conradi, Phys. Rev. Lett. **56**, 2284 (1986).
[30]L. J. Lewis and M. L. Klein, Phys. Rev. Lett. **57**, 2698 (1986).
[31]L. J. Lewis and M. L. Klein, J. Phys. Chem. **91**, 4990 (1987).
[32]L. J. Lewis and M. L. Klein, Phys. Rev. Lett. **59**, 1837 (1987).
[33]S. Galam, Phys. Lett. A **121**, 459 (1987).
[34]K. H. Michel, Phys. Rev. Lett. **57**, 2188 (1986); see also Phys. Rev. B **35**, 1405 (1987); **35**, 1414 (1987).
[35]J. O. Fossum and C. W. Garland, Phys. Rev. Lett. **60**, 592 (1988).
[36]L. J. Lewis and M. L. Klein, Phys. Rev. B **40**, 4877 (1989).
[37]J. Ihm, Phys. Rev. B **31**, 1674 (1985).
[38]M. Parrinello and A. Rahman, Phys. Rev. Lett. **45**, 1196 (1980).
[39]S. Nosé and M. L. Klein, J. Chem. Phys. **78**, 6928 (1983); Phys. Rev. Lett. **50**, 1207 (1983).

[40]R. W. Impey, S. Nosé, and M. L. Klein, Mol. Phys. **50**, 243 (1983).
[41]R. W. Impey, M. Sprik, and M. L. Klein, J. Chem. Phys. **83**, 3638 (1985).
[42]D. G. Bounds, M. L. Klein, I. R. McDonald, and Y. Ozaki, Mol. Phys. **47**, 629 (1982).
[43]D. G. Bounds, M. L. Klein, and I. R. McDonald, Phys. Rev. Lett. **46**, 1682 (1981).
[44]M. L. Klein and I. R. McDonald, J. Chem. Phys. **79**, 2333 (1983).
[45]M. Ferrario, I. R. McDonald, and M. L. Klein, J. Chem. Phys. **84**, 3975 (1986).
[46]P. W. Fowler and M. L. Klein, J. Chem. Phys. **85**, 3913 (1986).
[47]S. F. Edwards and P. W. Anderson, J. Phys. F **5**, 965 (1975).
[48]J. H. Walton and M. S. Conradi (unpublished); see also Bull. Am. Phys. Soc. **34**, 827 (1989).
[49]R. E. Wasylishen, B. A. Pettitt, and K. R. Jeffrey, J. Chem. Phys. **74**, 6022 (1981); R. E. Wasylishen and K. R. Jeffrey, *ibid.* **78**, 1000 (1983).